Stability of Brittle Fracture in Thermally Loaded Pressure Vessels

A. Carpinteri
(Istituto di Scienza delle Costruzioni),
M. Spiga
(Istituto di Fisica Tecnica)
Università di Bologna, Viale Risorgimento 2, I-40136 Bologna, Italy

Summary.

The integrity of the reactor pressure vessel is vital from a safety viewpoint. In fact, a massive failure of the reactor pressure vessel could damage the core seriously and break the containment. Thus, a single event could outflank the sequential barriers which prevent the escape of fission products in other accident sequences: the fuel cladding, the primary circuit and, should these fail, the containment building. Clearly, it is necessary to demonstrate that a disruptive and unstable failure of the reactor pressure vessel has a very low probability. Although a large loss-of-coolant accident (LOCA) results in a very rapid cool-down with high thermal stresses, the discharge of coolant reduces the internal over-pressure to essentially zero. Of greater concern with respect to pressure vessel integrity are those accidents which result in a rapid cool-down followed by a repressurising of the primary circuit to the normal operating pressures or slightly above. The cylindrical region of the vessel adjacent to the reactor core is fracture sensitive since it receives a high neutron flux which may result in some embrittlement of the material in this region. On the other hand, weld regions in the extreme areas are especially important because cracks or defects are likely to occur as a result of welding.

In the present paper, a thin-walled cylindrical pressure vessel of brittle material, fixed at the ends and containing a part-through circumferential surface crack, will be analyzed for loads generated by internal pressure and thermal gradient through the wall thickness.

It will be assumed that the wall thickness is so large that a condition of fully plastic cracked cross-section is to be excluded. Thus the stability of the fracture process will be studied assuming that the cracked section behaves as an elastic spring, rotating and extending under the actions of bending moment m and axial force f. Therefore three different local compliances will be defined: the rotational compliance λ_{mm}, the extensional compliance λ_{ff} and the mixed compliance $\lambda_{mf} = \lambda_{fm}$, simulating the vessel behaviour as if it were an equivalent cracked beam.

In this way it will be shown that the fracturing process tends to become stable by increasing the temperature level t and decreasing the gradient Δt (if the crack is at the external surface). The same criteria could be applied even in the case of real concrete pressure vessels [1] with ends fixed to hemispherical caps, in order to optimize the couple of design quantities t and Δt.

1. Simplified beam model.

Let us consider a thin-walled cylindrical pressure vessel of brittle material, fixed at the ends and containing a part-through circumferential surface crack (Fig. 1-a). Such a vessel is supposed to be loaded by the internal pressure p and by the thermal gradient $2\Delta t$ through the wall thickness h. If the thickness h is sufficiently thin with respect to the vessel radius R, the equivalent doubly fixed beam on the elastic foundation of stiffness $S = Eh/R^2$ (Fig. 1-b), may be considered constrained only at its ends. Then, the cracked section can be assumed to behave as an elastic spring, rotating and extending under the actions of bending moment m and axial force f. Three different local compliances will be defined (Fig. 1-c): the rotational compliance λ_{mm}, the extensional compliance λ_{ff} and the mixed compliance $\lambda_{mf} = \lambda_{fm}$, so that the displacement discontinuities at the cracked section can be expressed as follows [2][3]:

$$\Delta\phi = \lambda_{mm} m + \lambda_{mf} f \tag{1}$$

$$\Delta u = \lambda_{fm} m + \lambda_{ff} f \tag{2}$$

where ϕ is the rotation and u is the axial displacement. Therefore, the final statical scheme to be solved is a supported beam with an elastic spring at a distance x from the left end (Fig. 4-d), subjected to: the pressure p, the average temperature t, the temperature gradient $2\Delta t$, the redundant bending moments m_A and m_B, the redundant axial force f. In order to compute the three statically undefined reactions m_A, m_B and f, the three following equations of congruence will be imposed:

$$\phi_A = 0 \tag{3}$$

$$\phi_B = 0 \tag{4}$$

$$u_B = 0 \tag{5}$$

Finally, the crack tip stress-intensity factor K_I will be estimated by the relationship [2]:

$$K_I = \frac{m(x) Y_m(\xi)}{h^{3/2}} + \frac{f(x) Y_f(\xi)}{h^{1/2}} \tag{6}$$

where m(x) and f(x) are the internal loadings at the cracked section and the quantities Y_m and Y_f are functions of the relative crack depth ξ [2][3]:

$$Y_m(\xi) = 6 \times (1.99\ \xi^{1/2} - 2.47\ \xi^{3/2} + 12.97\ \xi^{5/2} - 23.17\ \xi^{7/2} + 24.80\ \xi^{9/2}) \tag{7}$$

$$Y_f(\xi) = 1.99\ \xi^{1/2} - 0.41\ \xi^{3/2} + 18.70\ \xi^{5/2} - 38.48\ \xi^{7/2} + 53.85\ \xi^{9/2} \tag{8}$$

Eqs. (7) and (8) are valid for $0 \leq \xi \leq 0.7$.

2. Solution of the problem.

Eqs. (3), (4) and (5) may be re-written as follows:

$$\frac{m_A \ell}{3EI} + \frac{m_B \ell}{6EI} - \frac{p\ell^3}{24EI} + \alpha\Delta t \frac{\ell}{h} + \phi_A(\Delta\phi) = 0 \tag{9}$$

$$-\frac{m_B \ell}{3EI} - \frac{m_A \ell}{6EI} + \frac{p\ell^3}{24EI} - \alpha\Delta t \frac{\ell}{h} + \phi_B(\Delta\phi) = 0 \tag{10}$$

$$\alpha t \ell + \frac{f\ell}{Eh} + u_B(\Delta u) = 0 \tag{11}$$

If the crack is always supposed to be in the stretched part of the beam, the displacements at the beam ends due to the distortions at the cracked section, are:

$$\phi_A(\Delta\phi) = -\Delta\phi\,\frac{\ell-x}{\ell} \tag{12}$$

$$\phi_B(\Delta\phi) = \Delta\phi\,\frac{x}{\ell} \tag{13}$$

$$u_B(\Delta u) = \Delta u \tag{14}$$

The discontinuities $\Delta\phi$ and Δu can be expressed by eqs. (1) and (2), the internal loadings being:

$$f(x) = f \tag{15}$$

$$m(x) = -m_A\,\frac{\ell-x}{\ell} - m_B\,\frac{x}{\ell} + \frac{1}{2}\,(p\ell x - px^2) \tag{16}$$

and the compliances:

$$\lambda_{mm} = \frac{2}{h^2E}\int_0^{\xi} Y_m^2(z)dz = \frac{2I_{mm}}{h^2E} \tag{17}$$

$$\lambda_{mf} = \lambda_{fm} = \frac{2}{hE}\int_0^{\xi} Y_m(z)Y_f(z)dz = \frac{2I_{mf}}{hE} \tag{18}$$

$$\lambda_{ff} = \frac{2}{E}\int_0^{\xi} Y_f^2(z)dz = \frac{2I_{ff}}{E} \tag{19}$$

Now, all the parameters involved in the analysis will be put into non-dimensional form, as reported in the Nomenclature. Eqs. (9), (10) and (11), in non-dimensional form, appear as follows:

$$C_{11}M_A + C_{12}M_B + C_{13}F = D_1 \tag{20}$$

$$C_{21}M_A + C_{22}M_B + C_{23}F = D_2 \tag{21}$$

$$C_{31}M_A + C_{32}M_B + C_{33}F = D_3 \tag{22}$$

where the coefficients C_{ij} are:

$$C_{11} = 1 + \frac{1}{2}\,H(1-X)^2I_{mm} \tag{23}$$

$$C_{12} = \frac{1}{2} + \frac{1}{2}\,HX(1-X)I_{mm} \tag{24}$$

$$C_{13} = 2(1-X)I_{mf} \tag{25}$$

$$C_{21} = -\frac{1}{2} - \frac{1}{2}\,HX(1-X)I_{mm} \tag{26}$$

$$C_{22} = -1 - \frac{1}{2}\,HX^2I_{mm} \tag{27}$$

$$C_{23} = 2XI_{mf} \tag{28}$$

$$C_{31} = -\frac{1}{2}\,H^2(1-X)I_{mf} \tag{29}$$

$$C_{32} = -\frac{1}{2}\,H^2XI_{mf} \tag{30}$$

$$C_{33} = 1 + 2HI_{ff} \tag{31}$$

and the known terms D_i are:

$$D_1 = P\left[\frac{1}{2H^3} + \frac{X(1-X)^2}{H^2}\,I_{mm}\right] - \frac{\Delta T}{H} \tag{32}$$

$$D_2 = -P\left[\frac{1}{2H^3} + \frac{X^2(1-X)}{H^2}\,I_{mm}\right] + \frac{\Delta T}{H} \tag{33}$$

$$D_3 = -P\,\frac{X(1-X)}{H}\,I_{mf} - T \tag{34}$$

Once eqs. (20), (21) and (22) have been solved, the dimensionless stress-intensity factor SIF $= K_I/h^{1/2}E$, is obtained from eq. (6):

$$SIF = \frac{H}{4} Y_m(\xi) \left[- M_A(1-X) - M_B X + P \frac{2X(1-X)}{H^3} \right] + F Y_f(\xi) \qquad (35)$$

3. Discussion.

Of the large number of possible parameter combinations, only a few can be discussed in the present section. We must keep in mind that positive values of function $K_I(\xi)$ mean that the crack is open (as has been hypothesized) and that negative values of function $K_I(\xi)$ mean that the crack is closed. Moreover, positive values of derivative $\partial K_I/\partial \xi$ mean unstable crack propagation, whereas negative values mean stable crack growth.

In Fig. 2, the dimensionless stress-intensity factor SIF is plotted against the relative crack depth ξ, by varying the dimensionless thickness H and for a dimensionless temperature gradient $\Delta T = 0.01$. In this case, pressure P and average temperature increase T are assumed to be equal to zero, while the crack is considered to be at the centre of the vessel and on the external surface.

The values of the stress-intensity factor are positive, i.e., the crack is open, since the external fibres are constrained by the hot internal fibres. It is interesting to observe that for small relative thicknesses the fracture process is always unstable, whereas for relative thicknesses higher than 0.05 the fracture process results to be stable after smaller and smaller crack lengths. When $H = 0.05$, the transition between unstability and stability occurs for $\xi = 0.57$, while, when $H = 0.10$, the transition occurs for $\xi = 0.47$. Therefore, it appears that the more flexible the system is, the more unstable the crack propagation is.

In Fig. 3, the same diagrams are reported when the crack is at the end of the vessel and on the external surface. Even in this case, for large relative thicknesses, the fracture process becomes stable. When $H = 0.05$, the transition occurs for $\xi = 0.42$, while, when $H = 0.10$, it occurs for $\xi = 0.28$. The crack stability is higher than in the preceding case because the crack is closer to the boundary, and then in a stiffer zone.

In Fig. 4, the stress-intensity factor is reported as a function of the crack depth ξ and varying the average temperature increase T, when the temperature gradient ΔT is 0.01 and the crack is at the centre. In this case, pressure P is considered equal to zero and a constant relative thickness $H = 0.01$ is assumed. For low T values the crack is open and always unstable. Then, increasing T, the crack tends to close and to be stable. The case $T = 0.005$ is remarkable, because it shows all three crack stages: open and unstable, open and stable, closed (and stable).

In Fig. 5, the same diagrams are reported when the crack is at the end of the vessel and on the external surface. Also in this case the interaction between temperature T and temperature gradient ΔT shows the same trends.

In Fig. 6, the stress-intensity factor is displayed against crack depth ξ by varying the dimensionless temperature gradient ΔT, when the crack is at the centre. In this case, pressure P is assumed equal to 10^{-4}, temperature T=0, relative thickness $H = 0.01$. The crack is always open and unstable. When the gradient ΔT is negative the crack tends to close. A value $\Delta T = -0.2$ is very close to annulling the pressure effect.

In Fig. 7, the same diagrams are proposed when the dimensionless crack distance from the end is $X = 0.3$. In this case, for $\Delta T = -0.2$, the crack is closed and the gradient effect prevails over the pressure effect. The criteria utilized in this paper are to be considered only as approximate methods in comparison with more sophisticated finite element analyses. Nevertheless, if we consider the large number of geometrical, mechanical and thermal varia-

bles involved in the problem, the presented solution may represent a useful and inexpensive way to predict the trends of the global vessel behaviour and to arrange for more refined investigations.

Nomenclature.

Dimensional quantities:

E	Young's modulus
f	axial force
h	vessel thickness
ℓ	vessel length
m	bending moment
p	internal pressure
R	vessel radius
t	average temperature
u	axial displacement
$2\Delta t$	temperature gradient
ϕ	rotation
λ	compliance
K_I	stress-intensity factor
x	distance of the crack from the vessel end

Dimensionless quantities:

H	$= h/\ell$
X	$= x/\ell$
ξ	= crack length/h
P	$= p/E$
T	$= \alpha t$
ΔT	$= \alpha \Delta t$
M	$= 4m\ell/h^3E$
F	$= f/hE$
SIF	$= K_I/h^{1/2}E$
I	= dimensionless compliance

References.

[1] CARPINTERI, A., "Application of fracture mechanics to concrete structures", Journal of the Structural Division, Proceedings of the American Society of Civil Engineers, Vol. 108, No. ST4, pp. 833-848, (1982).

[2] OKAMURA, H., WATANABE, K., TAKANO, T., "Applications of the compliance concept in fracture mechanics", American Society for Testing and Materials, Special Technical Publication, No. 536, pp. 423-438, (1973).

[3] OKAMURA, H., WATANABE, K., TAKANO, T., "Deformation and strength of cracked member under bending moment and axial force", Engineering Fracture Mechanics, Vol. 7, pp. 531-539, (1975).

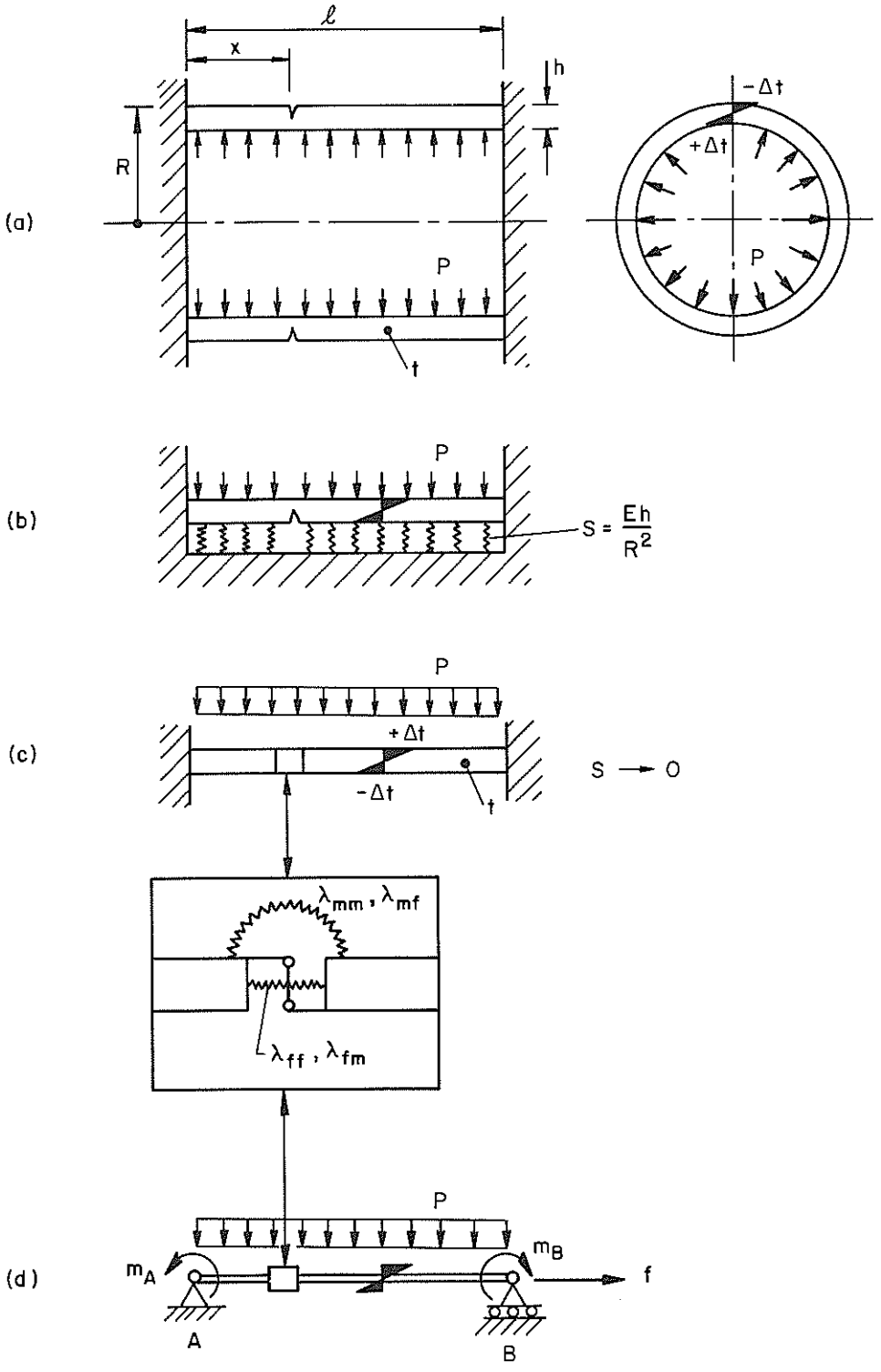

Fig. 1. Cylindrical pressure vessel containing a part-through circumferential crack.

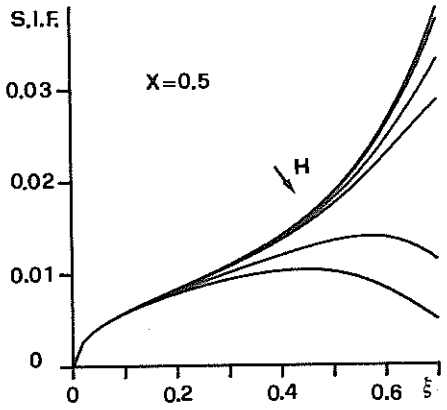

Fig. 2. Dimensionless stress-intensity factor versus crack depth at the centre of the vessel, for different values of H (10^{-5}, 10^{-3}, 5×10^{-3}, 10^{-2}, 5×10^{-2}, 10^{-1}) and $\Delta T = 0.01$, P=0, T=0.

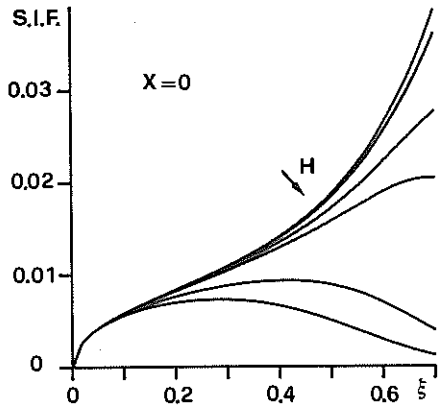

Fig. 3. Dimensionless stress-intensity factor versus crack depth at the end of the vessel, for different values of H (10^{-5}, 10^{-3}, 5×10^{-3}, 10^{-2}, 5×10^{-2}, 10^{-1}) and $\Delta T = 0.01$, P=0, T=0.

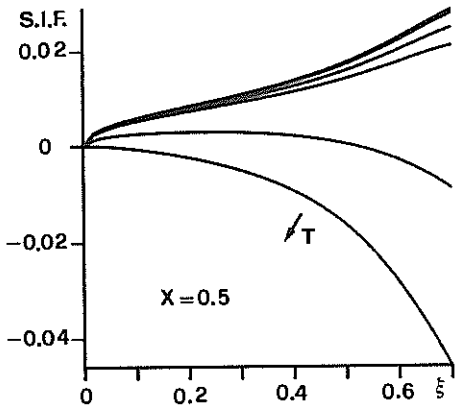

Fig. 4. Dimensionless stress-intensity factor versus crack depth at the centre of the vessel, for different values of T (0, 10^{-4}, 5×10^{-4}, 10^{-3}, 5×10^{-3}, 10^{-2}) and $\Delta T = 0.01$, P=0, H = 0.01.

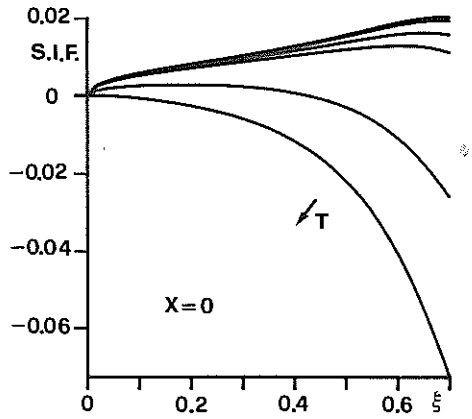

Fig. 5. Dimensionless stress-intensity factor versus crack depth at the end of the vessel, for different values of T (0, 10^{-4}, 5×10^{-4}, 10^{-3}, 5×10^{-3}, 10^{-2}) and $\Delta T = 0.01$, P=0, H = 0.01.

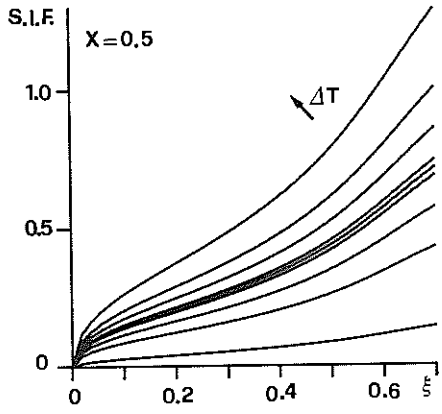

Fig. 6. Dimensionless stress-intensity factor versus crack depth at the centre of the vessel, for different values of ΔT (0, ±0.01, ±0.05, ±0.10, ±0.20) and $P = 10^{-4}$, T=0, H = 0.01.

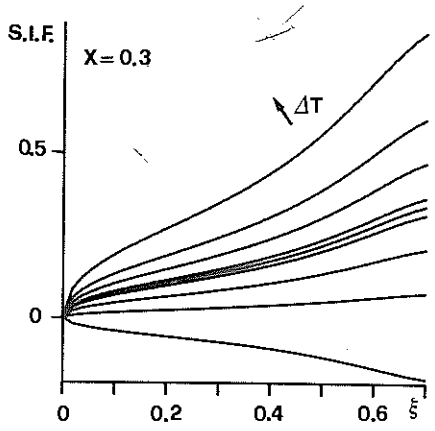

Fig. 7. Dimensionless stress-intensity factor versus crack depth in X = 0.3, for different values of ΔT (0, ±0.01, ±0.05, ±0.10, ±0.20) and $P = 10^{-4}$, T=0, H = 0.01.